


## Article

# Enhanced Pentostatin Production in *Actinomadura* sp. by Combining ARTP Mutagenesis, Ribosome Engineering and Subsequent Fermentation Optimization

Hongyu Zhang <sup>1</sup> , Deguang Zhang <sup>1</sup>, Ran Liu <sup>1</sup>, Tingting Lou <sup>2,\*</sup>, Ruyue Tan <sup>1</sup> and Suying Wang <sup>1,\*</sup>

<sup>1</sup> Tianjin Key Laboratory of Food Biotechnology, College of Biotechnology and Food Science, Tianjin University of Commerce, Tianjin 300134, China; zhanghongyu@tjcu.edu.cn (H.Z.); zdg1663754179@126.com (D.Z.); lr12340831@126.com (R.L.); z\_pillar@126.com (R.T.)

<sup>2</sup> Animal, Plant and Foodstuffs Inspection Center of Tianjin Customs, Tianjin 300461, China

\* Correspondence: loutingtingucas@126.com (T.L.); wsying@tjcu.edu.cn (S.W.)

**Abstract:** The special structure of pentostatin causes it to possess a wide spectrum of biological and pharmacological properties, and it has been extensively employed to treat malignant tumors and is the first-line treatment for hairy cell leukemia. Pentostatin is mainly distributed in several actinomycetes and fungi species. However, its low titer in microbes is not able to meet medical needs. Here, we report a strain improvement strategy based on combined atmospheric and room-temperature plasma (ARTP) mutagenesis and ribosome engineering screening, as well as fermentation optimization, for enhanced pentostatin production. The original strain, *Actinomadura* sp. ATCC 39365, was treated with ARTP and screened by ribosome engineering to obtain one stable pentostatin high-yield mutant *Actinomadura* sp. S-15, which produced 86.35 mg/L pentostatin, representing a 33.79% increase compared to *Actinomadura* sp. ATCC 39365. qRT-PCR analysis revealed that pentostatin biosynthesis-related gene expression was significantly upregulated in *Actinomadura* sp. S-15. Then, to further enhance pentostatin production, the fermentation medium was optimized in flask culture and the pentostatin production of *Actinomadura* sp. S-15 reached 152.06 mg/L, which is the highest pentostatin production reported so far. These results demonstrate the effectiveness of combined ARTP mutation, ribosome engineering screening, and medium optimization for the enhancement of pentostatin production, and provide a methodology enabling the sustainable production of pentostatin on an industrial scale.

**Keywords:** *Actinomadura* sp.; pentostatin; atmospheric and room temperature plasma; ribosome engineering



**Citation:** Zhang, H.; Zhang, D.; Liu, R.; Lou, T.; Tan, R.; Wang, S. Enhanced Pentostatin Production in *Actinomadura* sp. by Combining ARTP Mutagenesis, Ribosome Engineering and Subsequent Fermentation Optimization. *Fermentation* **2023**, *9*, 398. <https://doi.org/10.3390/fermentation9040398>

Academic Editor: Alexander A. Zhgun

Received: 24 March 2023

Revised: 16 April 2023

Accepted: 18 April 2023

Published: 20 April 2023



**Copyright:** © 2023 by the authors. Licensee MDPI, Basel, Switzerland. This article is an open access article distributed under the terms and conditions of the Creative Commons Attribution (CC BY) license (<https://creativecommons.org/licenses/by/4.0/>).

## 1. Introduction

Pentostatin, a purine antimetabolic drug, is the first-line treatment for hair-cell leukemia [1]. In 1991, the U.S. Food and Drug Administration (FDA) approved pentostatin injection for the treatment of acute T cell, chronic lymphocyte, and hair cell leukemia [2,3]. Pentostatin is mainly produced by microbial fermentation. It has been discovered in *Streptomyces antibioticus* NRRL 3238, *Actinomadura* sp. ATCC 39365, *Aspergillus nidulans*, *Cordyceps militaris*, and *Cordyceps kyushuensis Kobayasi*, in succession [4–8]. However, microbial-derived pentostatin has a low fermentation production, and the price remains high. To overcome the problem of low yield of pentostatin from microorganisms, hopes have been pinned on the chemical synthesis of pentostatin, but the chemical synthesis of pentostatin has presented serious disadvantages, such as long synthetic routes, harsh reaction conditions, very low production efficiency, high cost of consumption, and difficulty in achieving industrial production [9]. Therefore, research has been performed focusing on how to improve the fermentation production of pentostatin through biological means [10]. In a previous study, our research group tracked the pentostatin production of *Actinomadura* sp. ATCC 39365, but the low titer limits its adequate supply and has hampered efforts to perform further

preclinical studies or undertake clinical applications, and thus it fails to meet the high commercial requirements. Among currently available methods, rational metabolic engineering or genetic manipulation have great potential to boost the production of target compounds, but their successful application depends on a comprehensive knowledge of biosynthesis pathways and the amenability of the producers to carry out genetic modifications [11–13]. The pentostatin biosynthesis gene cluster has been identified in *Actinomadura* sp. ATCC 39365, but the genetic manipulation system of *Actinomadura* sp. ATCC 39365 has not been constructed. However, regarding industrial strains producing secondary metabolites like antibiotics, traditional and classical methods are still considered effective even without using genomic information or genetic tools [14]. Strain improvements through mutagenesis, including physical and chemical methods, are one of the most commonly used approaches for obtaining mutants with desirable biological and biotechnological traits [15–17].

Atmospheric room-temperature plasma (ARTP) is a novel mutagenesis technology that has been reported in recent years, which generates a plasma jet that can change the structure and permeability of the cell wall and plasma membrane and lead to DNA damage, including missense mutation, deletion, and nucleotide frameshift mutation [18]. Compared with the other conventional and typical mutation methods, ARTP has several advantages, such as nontoxicity, environmental friendliness, low cost, high efficiency and good repeatability [14]. ARTP mutagenesis technology has been employed for successful microbial breeding of bacteria, fungi, and microalgae, and hundreds of ARTP mutagenized strains have been reported to date [19–24]. ARTP mutagenesis can be combined with other conventional mutagenesis methods to obtain ideal strains more effectively [25,26]. Therefore, ARTP is considered to be one of the most efficient techniques for enhancing the productivity of the desired target product.

Ribosome engineering implements antibiotic-induced genetic mutations on various ribosome-associated factors like proteins and rRNA, consequently regulating gene expression and then affecting the metabolic network and the production of natural products [27,28]. Antibiotic-induced ribosome engineering could generate structural and functional variations of the ribosome and RNA polymerase, such as streptomycin and paromomycin resistance mutations at 30S ribosomal protein S12 (*rpsL* gene) [13,29], and rifamycin resistance mutation at RNA polymerase  $\beta$ -subunit (*rpoB* gene) [30,31], leading to transcriptional and translational modulations and consequently regulating the metabolic network to stimulate the production of secondary metabolites [32]. Hence, ribosome engineering has been regarded as an effective approach for achieving strain improvement and overproduction of various antibiotics and has been widely applied to increase the production of many industrially important antibiotics [32–41].

Herein, ARTP mutagenesis and ribosome engineering screening are integrated into the prescreening of high-yield pentostatin mutants followed by HPLC-MS/MS screening, aiding the rapid screening of high-pentostatin-titer mutants with high efficiency. Meanwhile, we elucidate the logical reason behind the improved performance of pentostatin biosynthesis mutants based on transcriptomic data analysis of the mutant and the original strain. Furthermore, fermentation optimization was conducted to sharply improve the pentostatin production of *Actinomadura* sp. S-15. The above facts indicate that pentostatin production can be significantly improved using the breeding strategy of ARTP mutagenesis and ribosome engineering screening, while the fermentation optimization method is also a useful addition. These results provide an effective bioengineering approach for improving pentostatin accumulation in rare actinomycetes.

## 2. Materials and Methods

### 2.1. Chemicals

Ultra-pure water (<5  $\mu\text{g/L}$  TOC) was obtained using an Avidity Cascada I (Jiaxing, Zhejiang, China) water purification system. Formic acid (puriss. p.a. for mass spectrometry) was obtained from China National Pharmaceutical Group Co., Ltd. (Shanghai, China). Methanol (HPLC grade) was obtained from Concord Technology Co., Ltd. (Tianjin, China).

Pentostatin standard with a purity higher than 98% was obtained from Aladdin Biochemical Technology Co., Ltd. (Shanghai, China). All culture medium components were obtained from Sangon Biotech Co., Ltd. (Shanghai, China).

## 2.2. Strains and Culture Conditions

The original strain *Actinomadura* sp. ATCC 39365 was obtained from the American Type Culture Collection (ATCC) and maintained in 10% glycerol at  $-80\text{ }^{\circ}\text{C}$ . *Actinomadura* sp. ATCC 39365 and its mutant were grown on ISP2 agar plates for sporulation. The mutants generated by ARTP mutagenesis and resistance screening were spread on ISP2 agar plates, activated in the ISP2 liquid seed medium, and fermented in a fermentation medium. The ISP2 liquid medium contained (g/L): glucose 4.0, malt extract 10.0, and yeast extract 4.0, pH = 7.8. For the ISP2 solid medium, 2% of agar was supplemented. The fermentation medium consisted of the following ingredients (g/L): glucose 4.0, malt extract 30.0, and yeast extract 12.0, pH = 7.8. All the media were autoclaved at  $115\text{ }^{\circ}\text{C}$  for 30 min before use. A total of 100  $\mu\text{L}$  spore suspension ( $10^8$  cells/mL) was inoculated in a 250 mL flask containing 30 mL fresh ISP2 medium and further incubated for 56 h as a seed culture medium. After that, the 5% inoculum was transferred into a 250 mL shake flask containing 30 mL fermentation medium and then incubated for 6–8 days in a rotary shaker at  $30\text{ }^{\circ}\text{C}$  with a shaking speed of 220 rpm.

## 2.3. Preparation of Single-Spore Suspension

*Actinomadura* sp. ATCC 39365 and its mutants were inoculated into ISP2 solid medium and incubated at  $28\text{ }^{\circ}\text{C}$  for 7 days. The mature spores were harvested using sterile cotton swabs scraped over the medium surface and then washed twice with sterile saline. The spore pellets were then transferred to an EP tube with glass beads, and the spore chains were disrupted by shaking for 10–30 min. After centrifuging at 12,000 rpm for 10 min and discarding the supernatant, the spore precipitate was carefully resuspended in 1 mL of sterile saline. The monospore suspension was counted using an Auvon Helber Bacteria Single Round Cell Thoma Counting Chamber and the concentration was adjusted to  $10^8$  cells/mL.

## 2.4. Random Mutagenesis by ARTP

ARTP mutagenesis was performed using the ARTP breeding system (ARTP-M, Yuan Qing Tian Mu Biotechnology Co., Ltd., Wuxi, China) in this study. The main parameters include power P ( $P = 130\text{ W}$ ), gas flow G ( $G = 10\text{ slm}$ ), the distance between the emission source and the carrier D ( $D = 2.0\text{ mm}$ ), and the temperature of the plasma T ( $T = 28\text{ }^{\circ}\text{C}$ ). For each ARTP mutagenesis, 10  $\mu\text{L}$  of the spore suspension (diluting to  $10^6$  cells/mL) was uniformly dispersed on a sterilized metal plate, and exposed to the ARTP jet for 0, 20, 40, 60, 80, 100, and 120 s, respectively. After mutagenesis with the selected exposure time, the cells were eluted with sterile saline into a 1.5 mL centrifuge tube. Cells were washed with fresh 0.85% sterile saline and recovered in 1.0 mL ISP2 medium and then incubated in a shaking incubator at  $30\text{ }^{\circ}\text{C}$  and 120 rpm for 4 h. Finally, 100  $\mu\text{L}$  of the diluent was cultivated on ISP2 agar plate for 5–7 days at  $30\text{ }^{\circ}\text{C}$ . For each exposure time, three replicate plates were set up. Then, the lethality rate of *Actinomadura* sp. ATCC 39365 under different ARTP treatment times was determined, and the lethality rate curve was obtained, as well as the desired exposure time. The individual colonies on the plates were counted manually, and the lethality (%) was determined using Equation (1).

$$\text{Lethality}(\%) = \frac{\text{Survival colonies} - \text{Survival colonies}}{\text{Survival colonies}} \times 100 \quad (1)$$

## 2.5. Resistant Screening of *Actinomadura* sp. ATCC 39365-Derived Mutants

To determine the minimum inhibitory concentration (MIC) of streptomycin, suspensions of the *Actinomadura* sp. ATCC 39365 spores (diluting to  $10^6$  cells/mL) were spread on ISP2 agar medium containing different concentrations of Str (5, 10, 20, 50, 100, and

200 µg/mL) and cultivated at 30 °C for observation. The MIC was defined as the minimum antibiotic concentration that fully inhibited the growth of the strain. Then, the spores were treated with ARTP, spread on the ISP2 medium agar plates containing streptomycin in different concentrations, and incubated at 30 °C for 6–8 days to obtain streptomycin resistance mutants, among which relatively large clones were picked out for further studies. Appropriate concentrations were used to select resistant mutants.

#### 2.6. Efficient Screening of Resistant Mutants with High-Yield Pentostatin by HPLC-MS/MS

Determination of pentostatin production was conducted by following procedures described previously [42]. After high-speed centrifugation, aqueous solution dilution, vortex shock, and microfiltration, the fermentation broth samples of the wild-type strain and mutants were analyzed by HPLC-MS/MS. The samples were separated on a Waters Atlantis T3 column (100 mm × 2.1 mm, 5 µm) by a gradient elution program using 10 mmol/L ammonium formate (containing 0.1% formic acid) and methanol (containing 0.02% formic acid) as mobile phases. Moreover, a chromatographic protection column (5 mm × 2.1 mm, 5 µm) was added to protect the column efficiency. The flow rate, column temperature, and injection volume were set at 0.3 mL/min, 25 °C, and 10 µL, respectively. The gradient elution procedure of the pentostatin is shown in Table 1, below: from 0 to 120 s, the ratio of mobile phase A (95%) and B (5%) remained unchanged; from 120 s to 480 s, the ratio of mobile phase A ranged from 95% to 5% and the ratio of mobile phase B ranged from 5% to 95%; from 480 s to 660 s, the ratio of mobile phase A ranged from 5% to 0% and the ratio of mobile phase B ranged from 95% to 100%; from 660 s to 1020 s, the ratio of mobile phase A ranged from 0% to 95% and the ratio of mobile phase B ranged from 100% to 5%.

**Table 1.** Gradient elution procedure of the pentostatin.

Time (s)	Flow Rate (mL/min)	φ(A)/%	φ(B)/%
0	0.3	95	5
120	0.3	95	5
360	0.3	5	95
180	0.3	0	100
360	0.3	95	5

φ(A): 10 mmol/L ammonium formate (0.1% formic acid); φ(B): methanol (0.02% formic acid).

#### 2.7. Verification of Genetic Stability of the Mutant with High-Yield Pentostatin

The genetic stability of the mutant strain was investigated by sub-culturing on plates for 6 passages. Then, the seed culture of the high-yield pentostatin mutant was transferred into the fermentation medium for 6–8 days, and the pentostatin production of each subculture was measured each day following fermentation in shake flasks.

#### 2.8. Determination of Biomass

The 30 mL of fermentation broth was placed in centrifuge tubes that were dried and weighed in advance. After centrifugation at 12,000 rpm for 5 min, the cells were washed with ultrapure water three times, and the precipitate was frozen under a temperature of −20 degrees; then, dry cell weight (DCW) was measured after drying to constant weight in a lyophilizer.

#### 2.9. qRT-PCR Analysis of Key Genes in the Biosynthesis Gene Cluster of Pentostatin

Fermentation culture broth (10 mL) of the resistant mutant and the parental strain *Actinomadura* sp. ATCC 39365 was centrifuged at 12,000 rpm for 15 min to collect mycelium cultured for 5 days and 8 days, respectively. Then, the total RNA was obtained using the UNIQ-10 Column Trizol Total RNA Isolation Kit (Sangon Biotech Co., Ltd., Shanghai, China) according to the manufacturer's instructions. The residual genomic DNA in the RNA sample was removed using RNase-free DNase I (Sangon Biotech Co., Ltd., Shanghai,

China). To verify the elimination of the residual DNA, the primers 16S-RT-F/16S-RT-R were used to amplify the total RNA. Reverse transcription-PCR (RT-PCR) was performed using Maxima Reverse Transcriptase (EP0743, Thermo Scientific) according to the instructions provided by the manufacturer. To analyze the transcriptional levels in the resistant mutant and the parental strain *Actinomadura* sp. ATCC 39365, quantitative real-time polymerase chain reaction (qRT-PCR) was conducted with ABI StepOnePlus™ Real-Time PCR System (ABI, Foster, CA, USA) according to the manufacturer's instructions. Six pairs of primers were used to determine the transcriptional levels of the key genes in the pentostatin biosynthesis gene cluster, including AdeA-F/AdeA-R, AdeB-F/AdeB-R, AdeC-F/AdeC-R, AdeK-F/AdeK-R, AdeM-F/AdeM-R, 16SrRNA-F/16SrRNA-R (Table 2). All the amplicons were confirmed by sequencing. The transcriptional levels were normalized using gene 16S rRNA as the internal control [43]. The fold changes in the test genes were quantified using the  $2^{-\Delta\Delta C_t}$  method [44]. Each qRT-PCR experiment was performed three times, and the error bar was used to show the standard deviations (SDs).

**Table 2.** Primers used for RT-qPCR genes.

Target Genes	Primer Sequence	T <sub>m</sub> (°C)
16S rRNA-F	5'-GAGCGAACAGGATTAGATACCC-3'	57.6
16S rRNA-R	5'-TCCTTTGAGTTTTAGCCTTGC-3'	57.2
Ade A-F	5'-GACTACCGGACCGACCCC-3'	59.4
Ade A-R	5'-GCCGAAGATGAGGCAGAAGT-3'	59.2
Ade B-F	5'-GTCATCACATGAGACCCCGG-3'	60.2
Ade B-R	5'-GAGCGGTCAGGGAGAAGAC-3'	60.1
Ade C-F	5'-GAGATCCCCCTGGTCGTC-3'	57.0
Ade C-R	5'-GCTCGGTGTTCTGGAGTAG-3'	58.0
Ade K-F	5'-ATCTCCAGCCTGGACGACCT-3'	62.5
Ade K-R	5'-CTAGGGCTCCGGTTTGC GTA-3'	62.0
Ade M-F	5'-CTCATGGTCCAGCTCGAAGG-3'	60.2
Ade M-R	5'-ATGACCTCGCAGAACACGTC-3'	60.4

### 2.10. Fermentation Optimization of the Mutant with High-Yield Pentostatin

To further improve the pentostatin production of the mutant strain, the fermentation conditions, including carbon sources, pH, culture time, and seed age were optimized. Based on the fermentation medium, the effects of various carbon sources on pentostatin production by mutant strain were evaluated. Five common carbon sources, including xylitol, maltitol, soluble starch, rice meal, and dextrin, were tested at concentrations of 4.0 g/L, with a constant malt extract and yeast extract of 10.0 g/L, pH = 7.8. After carbon sources had been assigned, the initial pH (6.9, 7.2, 7.5, 7.8, 8.1) of the fermentation medium, the seed age of transplantation (40 h, 48 h, 56 h, 64 h, 72 h, 80 h) and culture time (5 d, 6 d, 7 d, 8 d, 9 d) were investigated; the optimized fermentation parameters were used in subsequent fermentation studies. Each experiment on the optimization of carbon sources, pH, culture time, and seed age was performed in triplicate, and error bars show the standard deviations (SDs).

## 3. Results

### 3.1. Optimal ARTP Exposure Time on *Actinomadura* sp. ATCC 39365 Mutagenesis

For the effective mutation and screening of the mutants, it is desirable to have a high rate of cell lethality. After treatment with the ARTP plasma jet for 20 s, 40 s, 60 s, 80 s, and 100 s, the cells were incubated on ISP2 medium agar plates at 30 °C for 7 days, and the lethality rates of the treated spores increased to 51, 77, 90, 100, and 100%, respectively (Figure 1). No spores survived when the original strain *Actinomadura* sp. ATCC 39365 was treated for 80 s under these conditions. According to previous reports, a lethality rate of 90% can be regarded as appropriate [14,45]. Therefore, in this study, 60 s was selected as an appropriate exposure time for ARTP mutagenesis in which to obtain a desirable lethality rate.



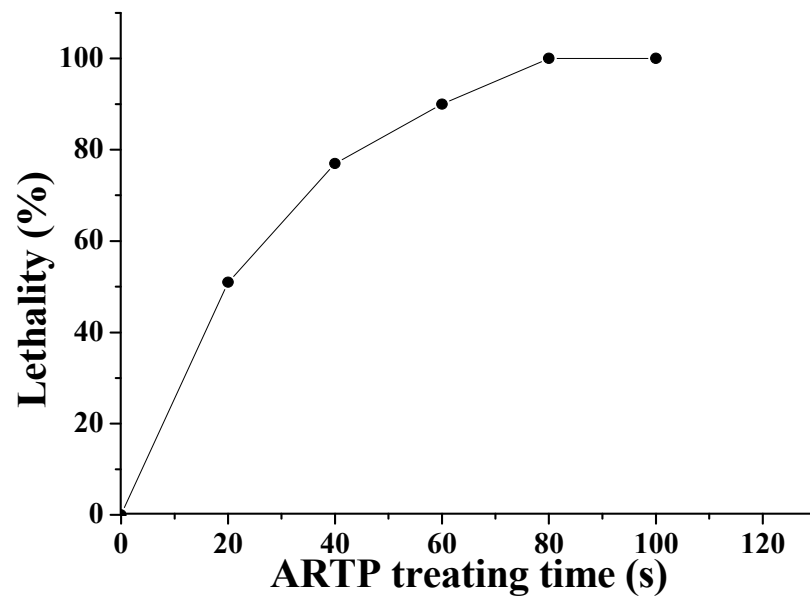


**Figure 1.** The lethality rate curves of *Actinomadura* sp. ATCC 39365 under ARTP mutagenesis.

### 3.2. Screening of High-Yield Pentostatin Mutants with Streptomycin

ISP2 medium agar plates containing 0, 5, 10, 15, 20, and 25 mg/L of streptomycin were prepared to determine the sensitivity of *Actinomadura* sp. ATCC 39365 to streptomycin. The lethality rates increased with increasing streptomycin concentration, reaching approximately 99.50% when the streptomycin concentration was 20 mg/L, the minimum inhibitory concentration of streptomycin for the *Actinomadura* sp. ATCC 39365 was 20 mg/L (Figure 2).

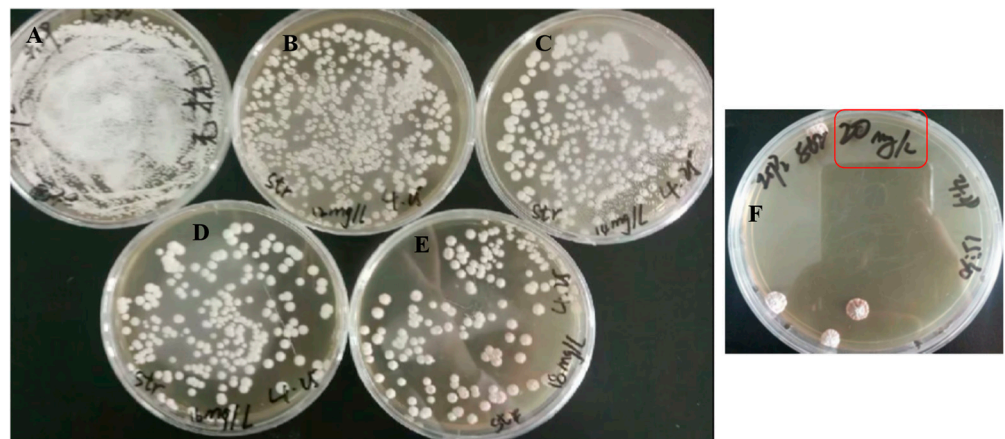


**Figure 2.** The MIC determination of streptomycin against *Actinomadura* sp. ATCC 39365. Different doses of streptomycin were added to the agar plates; the concentrations of streptomycin in plates (A–F) are 0, 12, 14, 16, 18 and 20 mg/L, respectively.

ISP2 plates containing 20 mg/L streptomycin (1xMIC) were used for the isolation of high-yield pentostatin mutants after ARTP mutagenesis. The mutants derived from streptomycin resistance screening after being cultivated on streptomycin-containing plates at different concentrations for 5–7 days are shown in Figure 3. Then, 100 relatively large ARTP mutant clones were selected to evaluate pentostatin production by cultivation in shake flasks, and 16 positive mutants showed higher pentostatin production than the original strain *Actinomadura* sp. ATCC 39365. Among them, the mutant *Actinomadura* sp. S-15 with the highest pentostatin production was chosen as being representative. The

mutant *Actinomadura* sp. S-15 showed the highest pentostatin production (86.35 mg/L), corresponding to a 33.79% increase compared with the wild-type strain (64.54 mg/L). The significant increase in pentostatin production confirmed that ARTP mutation breeding is an efficient method for generating high-yield mutants.

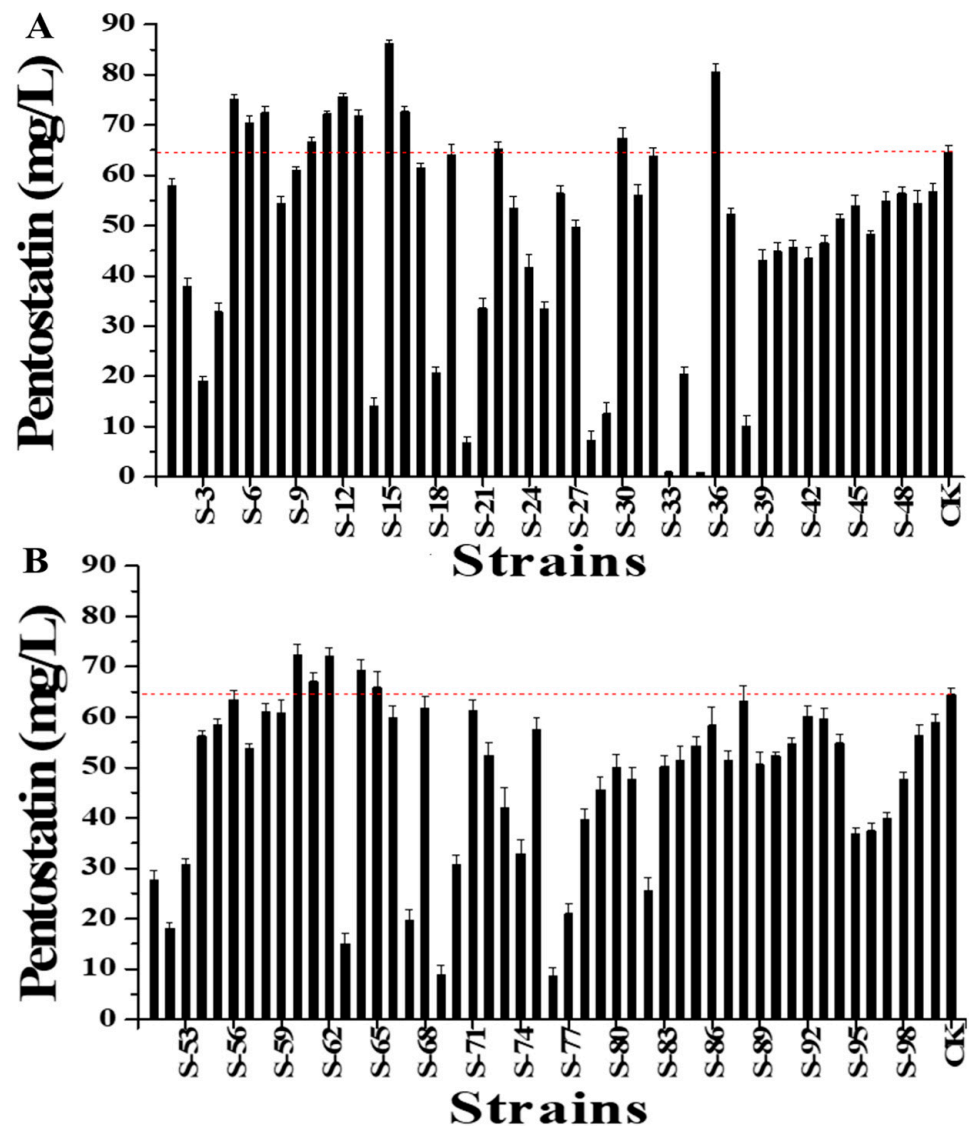


**Figure 3.** The pentostatin production of 100 mutants based on streptomycin screening. (A) The pentostatin production of mutants S-1 to S-50. (B) The pentostatin production of mutants S-51 to S-100. CK is the pentostatin production of control strain *Actinomadura* sp. ATCC 39365. The red dashed line is the dividing line based on the pentostatin yield of the negative control strain *Actinomadura* sp. ATCC 39365, and yields above the red dashed line are defined as high-yield mutants.

### 3.3. Genetic Stability of Mutant *Actinomadura* sp. S-15

The genetic stability of the mutant *Actinomadura* sp. S-15 was investigated by subculturing for six generations. Each generation of the strain was transferred into a fresh seed medium and then inoculated into a fermentation medium in shake flasks for 6 days. The results showed that the pentostatin production of these generations ranged from 83.26 to 83.96 mg/L (Figure 4), indicating no significant difference. This indicates that *Actinomadura* sp. S-15 is a genetically stable mutant strain that can be used for pentostatin production.

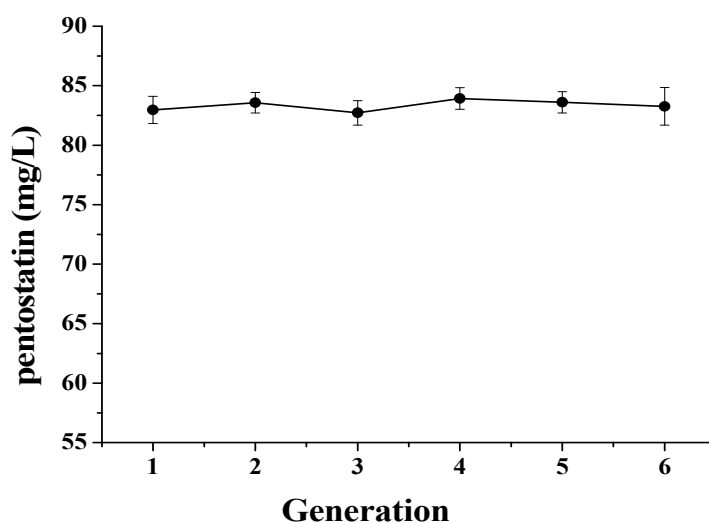


**Figure 4.** The genetic stability of the mutant *Actinomadura* sp. S-15 in six generations.

### 3.4. Transcription Levels of Key Genes Related to the Biosynthesis of Pentostatin

To understand the possible causes leading to improved production after ARTP mutation and ribosome screening, a transcriptional analysis of pentostatin biosynthesis-related genes was performed (Figure 5), with samples being collected at two time points, namely day 5 and day 8. Real-time PCR was carried out in triplicate for each sample, with 16S rRNA as an internal control. Firstly, RT-PCR was applied to determine co-transcription units in the gene cluster by amplifying the cDNA of *Actinomadura* sp. ATCC 39365 with primers. The genomic DNA of *Actinomadura* sp. ATCC 39365 was used as the control. As shown in Figure 5, there are totally eight co-transcription units in the pentostatin biosynthesis gene cluster, including AdeA-AdeC, AdeD-AdeE, AdeF-AdeJ, AdeK, AdeL-AdeM, AdeN-AdeT, AdeU, and AdeV [10]. To compare the relative expression levels of the pentostatin biosynthesis gene cluster in *Actinomadura* sp. S-15 and *Actinomadura* sp. ATCC 39365, qRT-PCR was then performed to analyze the samples collected on the 6th day and the 8th day, respectively. The key genes related to the pentostatin biosynthesis of AdeA, AdeB, AdeC, AdeK, and AdeM were selected to determine the corresponding expression levels. The results showed that the expression levels of AdeA, AdeB, AdeC, AdeK, and AdeM were higher in *Actinomadura* sp. S-15 than in the *Actinomadura* sp. ATCC 39365 (Tables S1 and S2). The upregulation of gene products included in these co-transcription units might lead to improved pentostatin production in *Actinomadura* sp. S-15.

### 3.5. Optimization of Fermentation Conditions of *Actinomadura* sp. S-15

To further improve pentostatin production, the effects of five carbon sources on pentostatin production were evaluated individually by replacing the carbon source (4 g/L glucose) in the original medium. The selected carbon sources included rice meal, dextrin, soluble starch, xylitol, and maltitol (all at concentrations of 4 g/L). The original medium served as a control. Other fermentation conditions, such as inoculum volume, the pH of the fermentation fluid, and culture time, remained unchanged, and each experiment was performed three times in parallel. As depicted in Figure 6, the biomass of *Actinomadura* sp. S-15 with different carbon sources ranged from 7.44 to 7.61 (mg/mL), indicating that there was no significant difference in mycelium growth. Nevertheless, in the medium containing maltitol, soluble starch, dextrin and rice meal, pentostatin production values were all higher than the control, and the highest pentostatin production of 98.97 mg/L was obtained with maltitol medium, a value which is 53.35% higher than that obtained in the original medium (64.54 mg/L) (Table S3, Figure 6A). Next, the effects of different maltitol concentrations on pentostatin production were studied (Table S4, Figure 6B). The results revealed increases in



production and biomass at a maltitol concentration of 4 g/L, with a maximum production of 96.21 mg/L.

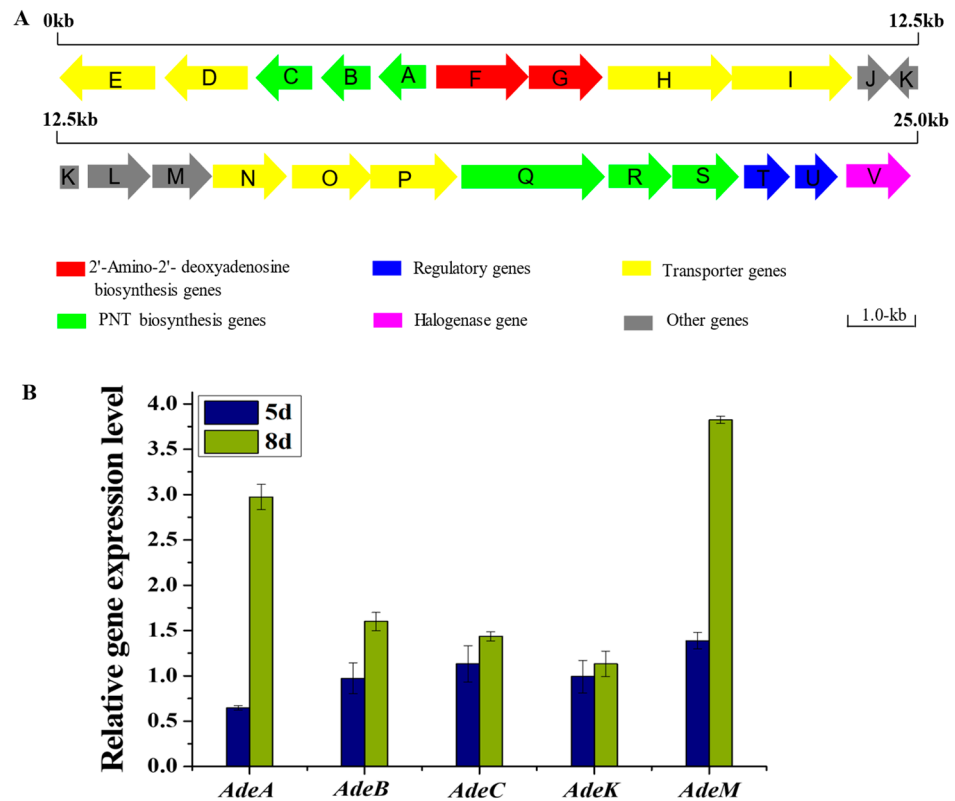


**Figure 5.** RT-qPCR analysis of the transcription levels of different genes in *Actinomadura* sp. S-15 and *Actinomadura* sp. ATCC 39365. (A) Genetic organization of co-transcription units in pentostatin biosynthetic gene cluster (*AdeA-AdeV*) [10]. (B) Relative expression levels of pentostatin biosynthesis gene cluster in *Actinomadura* sp. S-15, compared with those in *Actinomadura* sp. ATCC 39365. Five genes were selected to indicate the expression level of co-transcription units.

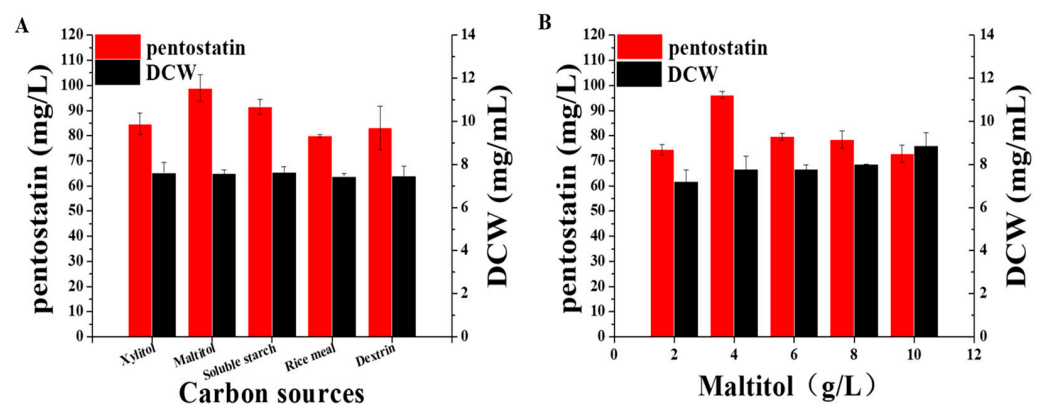


**Figure 6.** Effect of different carbon sources (A) and maltitol concentrations (B) on pentostatin production and biomass in *Actinomadura* sp. S-15.

The initial pH of the fermentation fluid affects the life activities of bacteria by changing their absorption of nutrients. When the carbon source of the fermentation liquid is changed, the pH changes accordingly. Therefore, by optimizing the type and concentration of carbon sources in the medium, the growth environment of the mutant strain could be improved by adjusting the initial pH of the fermentation medium, thus promoting pentostatin production. The results (Table S5, Figure 7A) showed that with increasing fermentation medium

initial pH, the pentostatin production and biomass of the mutant *Actinomadura* sp. S-15 first increased and then decreased. The pentostatin production and biomass of the mutant *Actinomadura* sp. S-15 reached their maximum values at a pH of 7.8, with a pentostatin production of 93.92 mg/L and a biomass of 7.87 mg/mL. Therefore, the initial pH of the fermentation medium was controlled at about 7.8.

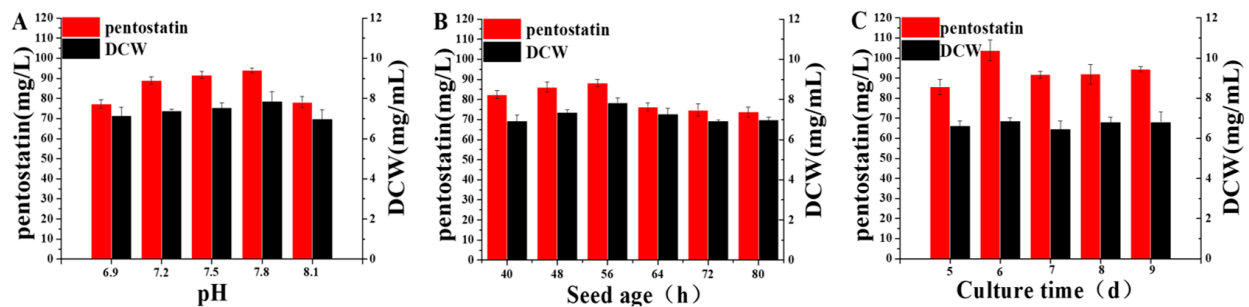


**Figure 7.** Effect of the initial pH of the fermentation medium (A), seed age (B) and culture time (C) on pentostatin production and biomass of *Actinomadura* sp. S-15.

The selection of a suitable seed age is very important for the fermentation process of high-yield mutants. During the seed liquid culture period, the growth vigor of the bacteria is strong and the delay period is short, such that bacteria are able to successfully survive the adaptation period. If the seed age is too young, the bacteria will grow slowly in the fermentation medium after inoculation, and the prolongation of culture time will also increase the probability of bacterial contamination. However, the bacteria will appear to age through autolysis and other phenomena if the seed liquid age is too great. Therefore, employing the optimized medium, the other culture conditions remained unchanged while optimizing the seed age. The results (Table S6, Figure 7B) showed that the mutant *Actinomadura* sp. S-15 demonstrated different pentostatin production levels with different seed ages. Pentostatin production and biomass reached their maximum values when the seed solution was inoculated for 56 h. Therefore, 56 h was chosen as the optimal seed age.

Using the optimized fermentation medium, the culture time was optimized while the other culture conditions remained unchanged. The results (Table S7, Figure 7C) showed that, with the change in the fermentation cycle, there were also fluctuations in the pentostatin production of the mutant *Actinomadura* sp. S-15. The pentostatin production and biomass of *Actinomadura* sp. S-15 reached their peak values when the fermentation cycle was 6 days. Therefore, under these conditions, the optimal culture time of the mutant *Actinomadura* sp. S-15 was 6 days.

After determining their optimal concentrations, the final production medium was simplified to contain 4 g/L maltitol, 30.0 g/L malt extract, and 12.0 g/L yeast extract, at pH = 7.8. The culture time used was 6 days, and the seed age was 56 h. Under these conditions, the average titer of pentostatin from different batches of flask fermentations improved sharply.

### 3.6. Difference in Fermentation Performance between *Actinomadura* sp. S-15 and *Actinomadura* sp. ATCC 39365

It was shown that, in 0–48 h, the biomass of the wild-type strain increased dramatically, the growth and reproduction of the strain were fast, and the metabolism was vigorous. From 48 h to 192 h, the biomass fluctuated slightly, but tended to be stable. The biomass of the mutant *Actinomadura* sp. S-15 increased rapidly from 0 to 24 h, and after 24 h, the trend was consistent with that shown by the wild-type strain, which tended to be stable. In conclusion, the mutant entered the stable phase 24 h earlier than the wild-type strain and entered the secondary metabolite synthesis stage in advance. The biomass of the mutant was greater than that of the wild-type strain. The maximum biomass of the mutant *Actinomadura* sp. S-15 was 8.20 mg/mL, which reached at 144 h, while the maximum

biomass of the wild-type strain *Actinomadura* sp. ATCC 39365 was 8.58 mg/L, which it reached at 192 h (Figure 8A).

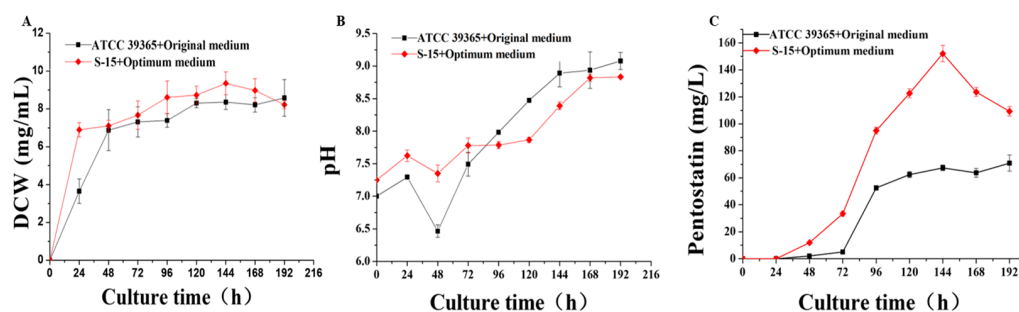


**Figure 8.** Differences in the fermentation performance with respect to biomass (A), pH (B) and pentostatin production (C) between *Actinomadura* sp. S-15 and *Actinomadura* sp. ATCC39365 in the original medium and optimum medium.

The pH of liquid fermentation showed a gradual rising trend during the fermentation process. During the period from 24 to 48 h, the pH of the fermentation medium decreased to varying degrees. It was speculated that the strain employed a large number of the nutrients in the medium and secreted acidic substances during the metabolic process. Since the same ventilation conditions were maintained for the strain throughout the culture process, the possibility that a change in ventilation conditions might result in incomplete oxidation was ruled out. After 48 h of fermentation, the pH increased gradually with increasing fermentation time, and both the wild-type strain and the mutant strain reached their maximum pH values at 192 h, and the difference between them was not obvious (Figure 8B).

As can be seen from the production curve of pentostatin (Figure 8C), the pentostatin production of the wild-type strain *Actinomadura* sp. ATCC39365 first increased and then stabilized. During the period between 72 and 96 h, the pentostatin production increased sharply, and during the period between 96 and 192 h, the pentostatin production stabilized, reaching its maximum at 192 h. The pentostatin production of the mutant *Actinomadura* sp. S-15 first increased and then decreased. According to the biomass curve, the mutant entered the stable growth stage at 24 h and began to produce a large number of secondary metabolites. From 24 h to 144 h, the pentostatin production increased sharply, and the maximum production of 152.06 mg/L was reached at 144 h. As shown in Figure 8, the mutants *Actinomadura* sp. S-15 showed a slight increase in biomass compared to the wild-type strain, while they showed a remarkable increase in pentostatin production.

#### 4. Conclusions

In this study, *Actinomadura* sp. ATCC 39365 was selected as the starting strain, and a pentostatin high-yield mutant *Actinomadura* sp. S-15 was obtained by atmospheric pressure and room-temperature plasma (ARTP) mutagenesis combined with the ribosome engineering screening strategy, which has application prospects for practical production. The pentostatin production and biomass of the mutant *Actinomadura* sp. S-15 and the starting strain *Actinomadura* sp. ATCC 39365 were systematically compared. By employing qRT-PCR, we were able to systematically analyze the genetic variations in the pentostatin high-yield mutant *Actinomadura* sp. S-15 and the starting strain *Actinomadura* sp. ATCC 39365 at the level of transcriptional changes in key genes related to the pentostatin biosynthesis gene cluster, and we performed a preliminary analysis of the high-yield mechanism. The fermentation parameters of the high-yield mutant *Actinomadura* sp. S-15 were optimized, and pentostatin production was greatly increased, reaching 152.06 mg/L. In addition, we finally obtained a high-yield pentostatin mutant *Actinomadura* sp. S-15 with good genetic stability. However, at present, the specific regulatory genes, global regulatory genes, and polymorphic regulatory genes in pentostatin biosynthesis are poorly

understood. In the future, bioinformatics methods could be used to analyze and predict its functions, to further increase the efforts of research on its rational modification, and improve pentostatin production from a molecular biology perspective. The fermentation parameter optimization in this paper was only conducted on a small scale in a shaker, the fermentation scale could be expanded and the fermentation effect could be verified in future studies.

**Supplementary Materials:** The following supporting information can be downloaded at: <https://www.mdpi.com/article/10.3390/fermentation9040398/s1>, Table S1: RT-qPCR analysis of the transcription levels of different genes in *Actinomadura* sp. S-15 compared with those in *Actinomadura* sp. ATCC 39365 on the 5th day; Table S2: RT-qPCR analysis of the transcription levels of different genes in *Actinomadura* sp. S-15 compared with those in *Actinomadura* sp. ATCC 39365 on the 8th day; Table S3: Effect of different carbon sources on pentostatin production and biomass in *Actinomadura* sp. S-15; Table S4: Effect of different maltitol concentrations on pentostatin production and biomass in *Actinomadura* sp. S-15; Table S5: Effect of the initial pH of the fermentation medium on pentostatin production and biomass of *Actinomadura* sp. S-15; Table S6: Effect of the seed age on pentostatin production and biomass of *Actinomadura* sp. S-15; Table S7: Effect of the culture time on pentostatin production and biomass of *Actinomadura* sp. S-15.

**Author Contributions:** H.Z. and D.Z.: writing—original draft, conceptualization, and visualization; T.L., R.L. and R.T.: writing—review and editing; S.W.: supervision and funding acquisition. All authors have read and agreed to the published version of the manuscript.

**Funding:** This project is funded by the 2021 Tianjin Graduate Research and Innovation Project under grant number 2021YJSS296 and Tianjin College Students Innovation and Entrepreneurship Training Program under grant number 202110069004.

**Institutional Review Board Statement:** Not applicable.

**Informed Consent Statement:** Not applicable.

**Data Availability Statement:** Not applicable.

**Conflicts of Interest:** The authors declare no conflict of interest.

## References

1. Gozzetti, A.; Sammartano, V.; Bacchiari, F.; Raspadori, D.; Bocchia, M. A BRAF-Negative Classic Hairy Cell Leukemia Patient with Long-Lasting Complete Remission after Rituximab and Pentostatin. *Turk. J. Hematol.* **2020**, *37*, 286–287. [CrossRef]
2. Ho, A.D.; Hensel, M. Pentostatin for the treatment of indolent lymphoproliferative disorders. *Semin. Hematol.* **2006**, *43*, S2–S10. [CrossRef]
3. Iannitto, E.; Tripodo, C. How I Diagnose and Treat Splenic Lymphomas. *Blood* **2011**, *117*, 2585–2595. [CrossRef]
4. Zhao, X.; Zhang, G.Y.; Li, C.Y.; Ling, J.Y. Cordycepin and Pentostatin Biosynthesis Gene Identified through Transcriptome and Proteomics Analysis of *Cordyceps kyushuensis* Kob. *Microbiol. Res.* **2019**, *218*, 12–21. [CrossRef]
5. Xia, Y.L.; Luo, F.F.; Shang, Y.F.; Chen, P.L.; Lu, Y.Z.; Wang, C.S. Fungal Cordycepin Biosynthesis is Coupled with the Production of the Safeguard Molecule Pentostatin. *Cell Chem. Biol.* **2017**, *24*, 1479–1489. [CrossRef]
6. Wu, P.; Wan, D.; Xu, G.; Wang, G.; Ma, H.; Wang, T.; Gao, Y.; Qi, J.; Chen, X.; Zhu, J.; et al. An Unusual Protector-Protege Strategy for the Biosynthesis of Purine Nucleoside Antibiotics. *Cell Chem. Biol.* **2017**, *24*, 171–181. [CrossRef]
7. Gao, Y.; Xu, G.; Wu, P.; Liu, J.; Cai, Y.S.; Deng, Z.; Chen, W. Biosynthesis of 2'-Chloropentostatin and 2'-Amino-2'-Deoxyadenosine Highlights a Single Gene Cluster Responsible for Two Independent Pathways in *Actinomadura* sp. Strain ATCC 39365. *Appl. Environ. Microbiol.* **2017**, *83*, e00078–e00087. [CrossRef]
8. Kodama, K.; Kusakabe, H.; Machida, H.; Midorikawa, Y.; Shibuya, S.; Kuninaka, A.; Yoshino, H. Isolation of 2'-Deoxycoformycin and Cordycepin from Wheat Bran Culture of *Aspergillus nidulans* Y 176–2. *Agric. Biol. Chem.* **1979**, *43*, 2375–2377. [CrossRef]
9. Truong, T.-V.; Rapoport, H. Chiroselective synthesis of the tetrahydroimidazodiaepinol aglycon of pentostatin and its analogues. *J. Org. Chem.* **1993**, *58*, 6090–6096. [CrossRef]
10. Zhang, H.; Liu, R.; Lou, T.; Zhao, P.; Wang, S.-Y. Pentostatin Biosynthesis Pathway Elucidation and Its Application. *Fermentation* **2022**, *8*, 459. [CrossRef]
11. Zhang, B.; Chen, Y.; Jiang, S.X.; Cai, X.; Huang, K.; Liu, Z.Q.; Zheng, Y.G. Comparative Metabolomics Analysis of Amphotericin B High-yield Mechanism for Metabolic Engineering. *Microb. Cell Fact.* **2021**, *20*, 66. [CrossRef]
12. Yin, S.; Wang, W.; Wang, X.; Zhu, Y.; Jia, X.; Li, S.; Yuan, F.; Zhang, Y.; Yang, K. Identification of a Cluster-situated Activator of Oxytetracycline Biosynthesis and Manipulation of Its Expression for Improved Oxytetracycline Production in *Streptomyces rimosus*. *Microb. Cell Fact.* **2015**, *14*, 46. [CrossRef]

13. Koshla, O.; Lopatniuk, M.; Borys, O.; Misaki, Y.; Kravets, V.; Ostash, I.; Shemediuk, A.; Ochi, K.; Luzhetskyy, A.; Fedorenko, V.; et al. Genetically Engineered rpsL Merodiploidy Impacts Secondary Metabolism and Antibiotic Resistance in *Streptomyces*. *World J. Microbiol. Biotechnol.* **2021**, *37*, 62. [[CrossRef](#)]
14. Zhang, K.; Mohsin, A.; Dai, Y.; Chen, Z.; Guo, M. Combinatorial Effect of ARTP Mutagenesis and Ribosome Engineering on an Industrial Strain of *Streptomyces albus* S12 for Enhanced Biosynthesis of Salinomycin. *Front. Bioeng. Biotechnol.* **2019**, *7*, 212. [[CrossRef](#)] [[PubMed](#)]
15. Huang, W.-W.; Ge, X.-Y.; Huang, Y.; Chai, X.-T.; Zhang, L.; Zhang, Y.-X.; Deng, L.-N.; Liu, C.-Q.; Xu, H.; Gao, J. High-yield Strain of Fusidic Acid Obtained by Atmospheric and Room Temperature Plasma Mutagenesis and the Transcriptional Changes Involved in Improving Its Production in Fungus *Fusidium coccineum*. *J. Appl. Microbiol.* **2021**, *130*, 405–415. [[CrossRef](#)] [[PubMed](#)]
16. Zhao, Y.; Song, Z.; Ma, Z.; Bechthold, A.; Yu, X. Sequential Improvement of Rimocidin Production in *Streptomyces rimosus* M527 by Introduction of Cumulative Drug-resistance Mutations. *J. Ind. Microbiol. Biotechnol.* **2019**, *46*, 697–708. [[CrossRef](#)] [[PubMed](#)]
17. Funane, K.; Tanaka, Y.; Hosaka, T.; Murakami, K.; Miyazaki, T.; Shiwa, Y.; Gibu, S.; Inaoka, T.; Kasahara, K.; Fujita, N.; et al. Combined Drug-Resistance Mutations Substantially Enhance Enzyme Production in *Paenibacillus agaridevorans*. *J. Bacteriol.* **2018**, *200*, e00188–18. [[CrossRef](#)]
18. Wang, X.-B.; Lu, M.-S.; Wang, S.-J.; Fang, Y.-W.; Wang, D.-L.; Ren, W.; Zhao, G.-M. The Atmospheric and Room Temperature Plasma (ARTP) Method on the Dextranase Activity and Structure. *Int. J. Biol. Macromol.* **2014**, *70*, 284–291. [[CrossRef](#)] [[PubMed](#)]
19. Ma, Y.; Yang, H.; Chen, X.; Sun, B.; Du, G.; Zhou, Z.; Song, J.; Fan, Y.; Shen, W. Significantly Improving the Yield of Recombinant Proteins in *Bacillus subtilis* by a Novel Powerful Mutagenesis Tool (ARTP): Alkaline  $\alpha$ -amylase as a Case Study. *Protein Expr. Purif.* **2015**, *114*, 82–88. [[CrossRef](#)] [[PubMed](#)]
20. Wang, Q.; Feng, L.R.; Wei, L.; Li, H.G.; Wang, L.; Zhou, Y.; Yu, X.B. Mutation Breeding of Lycopene-Producing Strain *Blakeslea Trispora* by a Novel Atmospheric and Room Temperature Plasma (ARTP). *Appl. Biochem. Biotechnol.* **2014**, *174*, 452–460.
21. Choi, J.I.; Yoon, M.; Joe, M.; Park, H.; Lee, S.G.; Han, S.J.; Lee, P.C. Development of Microalga *Scenedesmus Dimorphus* Mutant with Higher Lipid Content by Radiation Breeding. *Bioprocess Biosyst. Eng.* **2014**, *37*, 2437–2444. [[CrossRef](#)] [[PubMed](#)]
22. Qiu, L.; Nie, S.-X.; Hu, S.-J.; Wang, S.-J.; Wang, J.-J.; Guo, K. Screening of *Beauveria bassiana* with High Biocontrol Potential Based on ARTP Mutagenesis and High-throughput FACS. *Pestic. Biochem. Physiol.* **2021**, *171*, 104732. [[CrossRef](#)] [[PubMed](#)]
23. Dong, Y.; Liu, Y.; Lin, H.; Liu, C. Improving Vanadium Extraction from Stone Coal via Combination of Blank Roasting and Bioleaching by ARTP-mutated *Bacillus mucilaginosus*. *Trans. Nonferrous Met. Soc.* **2019**, *29*, 849–858. [[CrossRef](#)]
24. Yang, M.M.; An, Y.F.; Zayed, H.M.; Guoa, Q.; Yun, J.H.; Zhang, G.Y.; Awad, F.N.; Sun, W.J.; Qi, X.H. Random Mutagenesis of *Clostridium butyricum* Strain and Optimization of Biosynthesis Process for Enhanced Production of 1,3-propanediol. *Bioresour. Technol.* **2019**, *284*, 188–196. [[CrossRef](#)]
25. Wei, L.; Mao, Y.; Liu, H.; Ke, C.; Liu, X.; Li, S. Effect of an Inorganic Nitrogen Source  $(\text{NH}_4)_2\text{SO}_4$  on the Production of Welan gum from *Sphingomonas* sp. Mutant Obtained through UV-ARTP Compound Mutagenesis. *Int. J. Biol. Macromol.* **2022**, *210*, 630–638. [[CrossRef](#)]
26. Yun, J.; Zayed, H.-M.; Zhang, Y.; Zhang, G.; Zhao, M.; Qi, X. Improving Tolerance and 1,3-propanediol Production of *Clostridium butyricum* Using Physical Mutagenesis, Adaptive Evolution and Genome Shuffling. *Bioresour. Technol.* **2022**, *363*, 127967. [[CrossRef](#)]
27. Ochi, K.; Okamoto, S.; Tozawa, Y.; Inaoka, T.; Hosaka, T.; Xu, J.; Kurosawa, K. Ribosome Engineering and Secondary Metabolite Production. *Adv. Appl. Microbiol.* **2004**, *56*, 155–184.
28. Ochi, K.; Okamoto, S. New Development to Utilize *Streptomyces* by “Ribosome Engineering”. *Nippon. Nogeikagaku Kaishi J. Agric. Chem. Soc. Jpn.* **2004**, *78*, 1082–1085. [[CrossRef](#)]
29. Okamoto-Hosoya, Y.; Sato, T.A.; Ochi, K. Resistance to Paromomycin is Conferred by rpsL Mutations, Accompanied by an Enhanced Antibiotic Production in *Streptomyces coelicolor* A3(2). *J. Antibiot.* **2000**, *53*, 1424–1427. [[CrossRef](#)]
30. Kim, H.; Kim, S.H.; Ying, Y.H.; Kim, H.J.; Koh, Y.H.; Kim, C.J.; Lee, S.H.; Cha, C.Y.; Kook, Y.H.; Kim, B.J. Mechanism of Natural Rifampin Resistance of *Streptomyces* spp. *Syst. Appl. Microbiol.* **2005**, *28*, 398–404. [[CrossRef](#)]
31. Nguyen, C.T.; Dhakal, D.; Pham, V.T.; Nguyen, H.T.; Sohng, J.K. Recent Advances in Strategies for Activation and Discovery/Characterization of Cryptic Biosynthetic Gene Clusters in *Streptomyces*. *Microorganisms* **2020**, *8*, 616. [[CrossRef](#)]
32. Zhu, S.B.; Duan, Y.W.; Huang, Y. The Application of Ribosome Engineering to Natural Product Discovery and Yield Improvement in *Streptomyces*. *Antibiotics* **2019**, *8*, 133. [[CrossRef](#)] [[PubMed](#)]
33. Tanaka, Y.; Kasahara, K.; Izawa, M.; Ochi, K. Applicability of Ribosome Engineering to Vitamin B12 Production by *Propionibacterium shermanii*. *Biosci. Biotechnol. Biochem.* **2017**, *81*, 1636–1641. [[CrossRef](#)]
34. Lv, X.A.; Jin, Y.Y.; Li, Y.D.; Zhang, H.; Liang, X.L. Genome Shuffling of *Streptomyces viridochromogenes* for Improved Production of Avilamycin. *Appl. Microbiol. Biotechnol.* **2013**, *97*, 641–648. [[CrossRef](#)] [[PubMed](#)]
35. Yu, G.; Hui, M.; Li, R.; Chen, L.; Tian, H.; Wang, L. Enhancement of Daptomycin Production by the Method of Combining Ribosome Engineering and Genome Shuffling in *Streptomyces roseosporus*. *Appl. Biochem. Microbiol.* **2018**, *54*, 611–615. [[CrossRef](#)]
36. Liu, H.M.; Jiang, C.Z.; Lin, J.; Zhuang, Z.K.; Kong, W.P.; Liu, L.; Huang, Y.; Duan, Y.W.; Zhu, X.C. Genome Shuffling Based on Different Types of Ribosome Engineering Mutants for Enhanced Production of 10-membered Eneidyne tiancimycin-A. *Appl. Microbiol. Biotechnol.* **2020**, *104*, 4359–4369. [[CrossRef](#)]



37. Zhu, X.C.; Kong, J.Q.; Yang, H.; Huang, R.; Huang, Y.; Yang, D.; Shen, B.; Duan, Y.W. Strain Improvement by Combined UV Mutagenesis and Ribosome Engineering and Subsequent Fermentation Optimization for Enhanced 6'-deoxy-bleomycin Z Production. *Appl. Microbiol. Biotechnol.* **2018**, *102*, 1651–1661. [[CrossRef](#)]
38. Tong, Q.-Q.; Zhou, Y.-H.; Chen, X.-S.; Wu, J.-Y.; Wei, P.; Yuan, L.-X.; Yao, J.-M. Genome Shuffling and Ribosome Engineering of *Streptomyces virginiae* for Improved Virginiamycin Production. *Bioprocess Biosyst. Eng.* **2018**, *41*, 729–738. [[CrossRef](#)]
39. Li, Y.M.; Li, J.Y.; Ye, Z.M.; Lu, L.C. Enhancement of Angucycline Production by Combined UV mutagenesis and Ribosome Engineering and Fermentation Optimization in *Streptomyces dengpaensis* XZHG99(T). *Prep. Biochem. Biotechnol.* **2021**, *51*, 173–182. [[CrossRef](#)]
40. Ochi, K. Insights into Microbial Cryptic Gene Activation and Strain Improvement: Principle, Application and Technical Aspects. *J. Antibiot.* **2017**, *70*, 25–40. [[CrossRef](#)]
41. Lee, J.; Kim, D.-S.; Jewett, M.-C. 6.17-Recent Advances in Engineering Ribosomes for Natural Product Biosynthesis. *Compr. Nat. Prod. III* **2020**, *6*, 377–397.
42. Zhao, M.; Zhang, H.; Lou, T.; Zhao, K.; Wang, S. Simultaneous Determination of Pentostatin and 2'-amino-2'-deoxyadenosine in Fermentation Broth by High Performance Liquid Chromatography-tandem Mass Spectrometry. *Se Pu* **2021**, *39*, 744–749. [[CrossRef](#)] [[PubMed](#)]
43. Wang, W.-Y.; Yang, S.-B.; Wu, Y.-J.; Shen, X.-F.; Chen, S.-X. Enhancement of A82846B Yield and Proportion by Overexpressing the Halogenase Gene in *Amycolatopsis orientalis* SIPI18099. *Appl. Microbiol. Biotechnol.* **2018**, *102*, 5635–5643. [[CrossRef](#)] [[PubMed](#)]
44. Livak, K.-J.; Schmittgen, T.-D. Analysis of Relative Gene Expression Data Using Real-Time Quantitative PCR and the  $2^{-\Delta\Delta CT}$  Method. *Methods* **2001**, *25*, 402–408. [[CrossRef](#)]
45. Ma, X.-J.; Zhang, H.-M.; Lu, X.-F.; Han, J.; Zhu, H.-X.; Wang, H.; Yao, R.-S. Mutant Breeding of *Starmerella bombicola* by Atmospheric and Room-temperature Plasma (ARTP) for Improved Production of Specific or Total Sophorolipids. *Bioprocess Biosyst. Eng.* **2020**, *43*, 1869–1883. [[CrossRef](#)]

**Disclaimer/Publisher's Note:** The statements, opinions and data contained in all publications are solely those of the individual author(s) and contributor(s) and not of MDPI and/or the editor(s). MDPI and/or the editor(s) disclaim responsibility for any injury to people or property resulting from any ideas, methods, instructions or products referred to in the content.